

Development of a Maglev LCD Glass Conveyor

Chang-Hyun Kim, Jong-Min Lee, and Hyung-Suk Han

Korea Institute of Machinery & Materials, 104 Sinseongno, Yuseong-gu, Daejeon, 305-343, Korea

chkim78@kimm.re.kr, lee_jm@kimm.re.kr, hshan@kimm.re.kr

Chang-Woo Lee

Evertchno Co., LTD, 139-1 Sandongri, Eumbongmyun, Asan-City, Chungcheongnam-do, 226-863, Korea

leecw@evertchno.co.kr

ABSTRACT: In this paper, the development of a maglev LCD glass conveyor is presented. Both electromagnets (EM) and permanent magnets (PM) are used for levitation. PMs are used to reduce the overall power consumption. A linear induction motor (LIM) is adopted for thrust and an optical barcode positioning system is used to obtain the absolute position of the vehicle. Power is delivered by a contactless power supply (CPS), hence the vehicle is working completely contactless. Due to the contactless design, the system generates no particle and an improved production yield is expected. The electromagnets are controlled to maintain a constant air gap, and position control of the LIM is implemented with velocity profile generation. Simulations and experiments have been carried out to show the performances of the levitation and position control.

1 INTRODUCTION

Due to an increasing demand for larger displays, the manufacturing facility is also getting larger and larger. Noise, vibration and airborne particles are often problematic with the conventional manufacturing facility, and the need for a new manufacturing system has been arisen to overcome these shortcomings. Non-contact operation is essential for this purpose, and a magnetically levitated suspension gains much attention in semiconductor and display industries.

In this paper, a magnetically levitated LCD glass conveyor has been developed. Permanent magnets are used to reduce required power consumption (Kim et al. 2011, Kim et al. 2001, Mizuno & Takemori 2002, Morishita et al. 1989, Sun & Oka 2009, Tzeng & Wang 1995). Due to the contactless design, the system generates no particle and an improved production yield is expected.

The organization of this paper is as follows. In section 2, the structure and the design of the developed system are described. In section 3, the control architecture and its implementation will be explained. In section 4, simulations and experimental results will be given to show the levitation and position control performances. Finally, some concluding remarks will be presented in section 5.

2 SYSTEM DESIGN OF A MAGLEV LCD GLASS CONVEYOR

2.1 Structure of the Maglev LCD glass conveyor

The system design is mainly related with levitation and thrust mechanisms. Figure 1 shows the sectional view of the conveyor vehicle. The configuration is similar to the previous maglev train of which rail structure is surrounded by the levitation support. To decrease power consumption, permanent magnets (PM) as well as electromagnets (EM) are used to lift the vehicle. Two linear induction motors (LIM) are installed on the upper side of the rail to thrust the vehicle by the electromagnetic induction force. Power is supplied with no contact from contactless power supply (CPS) cables in the middle of the vehicle. And, vertical and lateral guide rollers are installed to prevent the collision between the vehicle and the rail. Figure 2 shows the constructed LCD glass conveyor system and its components.

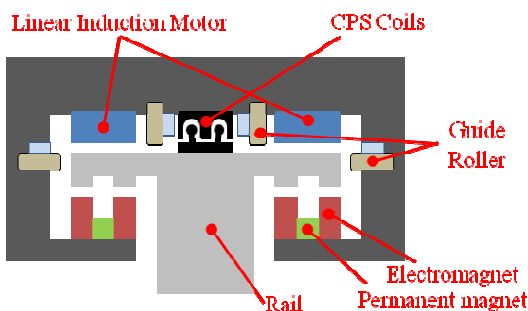


Figure 1. Sectional view of the conveyor vehicle.

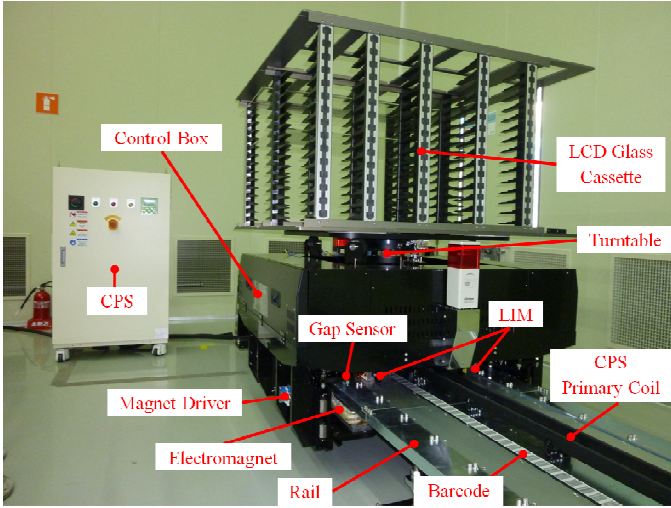


Figure 2. Maglev LCD glass conveyor.

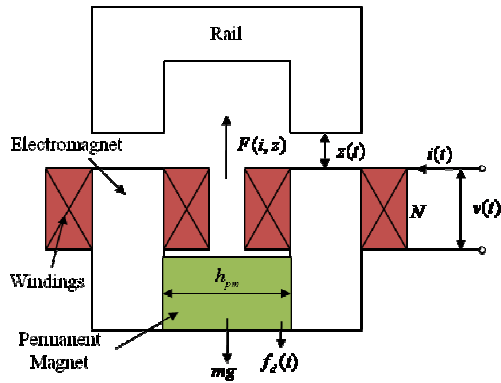


Figure 3. Simplified levitation model.

2.2 Design of the levitation and thrust systems

Figure 3 shows the cross-sectional view of the simplified levitation EM. The EM has a U-shaped ferromagnetic body and the PM is inserted in the middle of the electromagnet. The levitation system consists of eight same EMs, and two EMs are placed at each corner of the vehicle. Before the design process, the mathematical model of the EM is derived. In figure 3, z denotes the length of airgap, f_d is the disturbance force, and i is the current of coils. The flux density in the air gap can be written as

$$B = \frac{\phi_g}{A_g} = \frac{ai + B_r}{bz + 1} \quad (1)$$

where A_g is the area of the pole, and $B_r = 1.23$ is the residual flux density of the PM. And the coefficients are defined as

$$a = \frac{\mu_{pm}\mu_0 N}{h_{pm}} = \frac{1.05\mu_0 N}{h_{pm}} \quad (2)$$

$$b = \frac{2\mu_{pm}}{h_{pm}} \quad (3)$$

where μ_0 is the permeability of the air, μ_{pm} the relative permeability of the PM, h_{pm} the height of the PM, and N is the number of coil turns.

Then, the attraction force can be written as

$$F(i(t), z(t)) = -\frac{\partial W(t)}{\partial z(t)} = \frac{A_g}{\mu_0} B(t)^2 = \frac{A_g}{\mu_0} \left\{ \frac{ai(t) + B_r}{bz(t) + 1} \right\}^2 \quad (4)$$

The levitation system consists of eight EMs placed at four corners of the vehicle and is initially designed to lift a 750-kg mass including 350-kg load. Table 1 shows the important specifications of the designed levitation EM. The nominal gap is 3mm and the computed levitation force of eight EMs at the nominal gap is 760.9kg.

Table 1. Specifications of levitation electromagnet.

Items	Value
Pole dimension	200×20×60(L×W×Hmm3)
Total weight	75.0kg
Initial gap	5mm
Nominal gap	3mm
Maximum current	±10A
Levitation weight	760.9kg(@0A, gap=3mm)

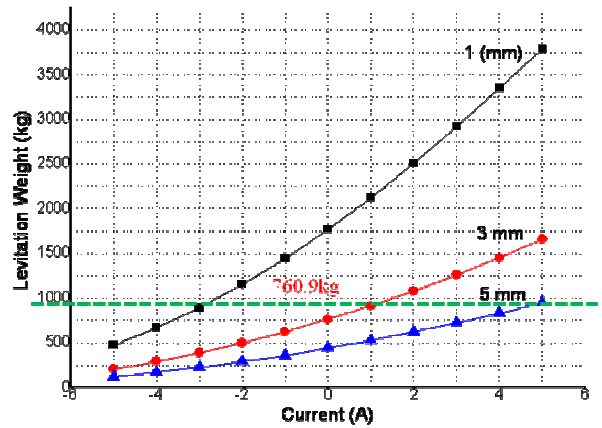


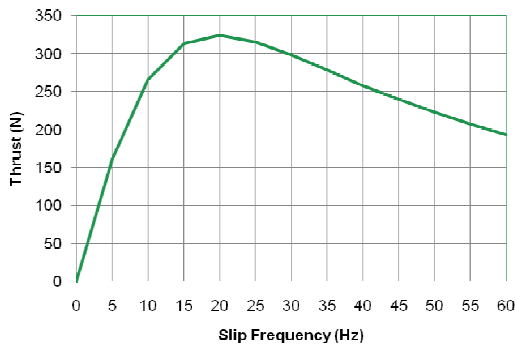
Figure 4. Levitation force vs. coil current.

Generally, the theoretical force in (4) is quite different from the actual force due to the effects of leakage flux, Eddy current loss, magnetization and so on. 3-Dimensional finite element analysis (FEA) can provide more realistic results in this case. Figure 4 shows the estimated levitation force according to the current and gap variations using FEA. In this figure, assume that the total weight of the vehicle is 760.9kg, the attraction force more than 760.9kg can be

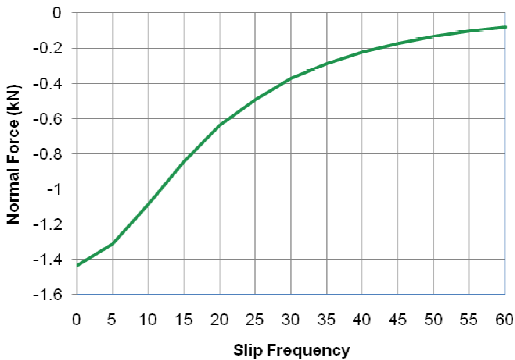
generated by supplying 5A to the coil in order to levitate the vehicle at the landing position (5mm gap). And, the attraction force is less than 760.9kg by providing -3A to the coil in order to separate the vehicle from the rail at the stuck position (1mm gap). Therefore, the levitation control of a 760.9-kg vehicle can be achieved with supplying currents within $\pm 5A$.

A thrust system consists of two LIMs, aluminum sheets, and the rail. Two LIMs are placed in left and right sides of the vehicle. The LIM has 3-phase primary winding embedded in the LIM core on the vehicle, and the aluminum sheet and steel rail form the secondary circuit of the motor. A new LIM is designed for the conveyor system and the expected performance curves of the designed LIM are shown in Figure 5.

The thrust and normal forces at the nominal gap (3mm), the nominal current (10A), and the slip frequency (around 20Hz) are estimated as 323N and 640N, respectively. Then, overall forces are twice of the estimated values because two LIMs are installed on the conveyor vehicle. Important specifications of the designed LIM are listed in Table 2.



(a) Performance curve of thrust force.



(b) Performance curve of normal force.

Figure 5. Performance curves of the designed LIM.

Table 2. Specifications of linear induction motor.

Items	Value
Power	220V, 10A(3-phase)
Number of poles	8
Thrust force	323N
Normal force	640N

3 CONTROL OF A MAGLEV LCD GLASS CONVEYOR

3.1 Control architecture

To operate levitation and thrust system of the maglev LCD glass conveyor, some components such as power electronics and sensors are needed. For levitation control, the gap between the levitation magnet and the rail is measured by gap sensors and is controlled to maintain a constant air gap. For thrust control, the absolute position of the conveyor is recognized by a barcode positioning system and the conveyor is controlled to stop at the desired position.

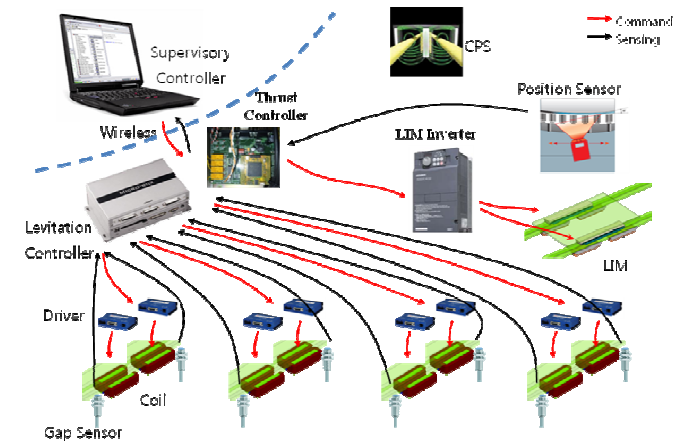


Figure 6. Control architecture and signal flows.

Figure 6 shows the control architecture of the conveyor system and its signal flows. There are two independent controllers for levitation and thrust, and a supervisory controller outside of the conveyor, which is responsible for task scheduling, transmits commands via bluetooth wireless communication. Main power is provided by CPS, hence the conveyor is working completely contactless.

Totally eight levitation EMs are used and a pair of EMs are placed at each corner, and two gap sensors are used together for one corner. The reason why two gap sensors are combined is to compensate false readings of the gap sensor at rail joints. Two gap sensors are located at the front and rear sides of each pair of magnets. Eight EMs are driven by eight current drivers, and each pair of EMs is commanded with the same current reference.

A barcode tape is attached along the rail and the absolute position of the conveyor is obtained by a barcode reader, of which accuracy is up to 0.1 mm. Two LIM are driven by a vector control inverter.

3.2 Levitation control

The dynamic equation of the levitation system is as follows:

$$m \frac{d^2 z(t)}{dt^2} = mg + f_d(t) - F(i(t), z(t)) \quad (5)$$

where m is the weight of the levitated object and g is the acceleration due to gravity. Above model is used in the simulation and the controller is designed based on this model.

The first step of levitation control is the measurement of gap signals. As mentioned before, the gap sensor gives a false reading that is 0.5mm less than the actual value at the rail joint and this error should be compensated properly (Sung et al. 2006). Two sensors are used for a pair of EMs and the actual gap is estimated by several combinations based on the difference between two gap measurements. In addition, a low pass filter is adopted to reduce sensor noises.

The controller is based on the conventional phase lead-lag compensator in continuous time domain and discretized using the bilinear transform. In addition, zero-power control (Sun & Oka 2009) is applied to balance the attraction force and the total weight.

The simulation and control program for levitation is implemented with MATLAB and Simulink to facilitate Rapid Prototyping, a process that allows block diagram modeling and provides a preview of system performance prior to final implementation. Using MATLAB's Real-Time Workshop and xPC Target, the program code of control block diagram can be generated, compiled, downloaded, and run on MicroBox automatically. Tedious, time-consuming debugging can be avoided and total development time can be saved. TeraSoft's MicroBox, which is a small fanless industrial PC with 1 GHz Intel's Celeron M CPU, is used as a levitation controller. It has 8-channel 16-bit ADC and 4-channel 16-bit DAC to interface with sensors and current drivers.

3.3 Position control

The position controller receives the absolute position of the conveyor vehicle from the barcode reader, and makes the vehicle stop at the desired position. The barcode reader gives the position measurement via either serial communication or an encoder interface, and the position controller provides reference velocity commands to the LIM inverter.

The position controller was developed using Texas Instruments's floating point DSP. The position controller has several peripherals such as serial communication interfaces, encoder interfaces, DAC,

ADC and relay interfaces. The position controller also re-transmits the command, which is received from the supervisory controller via wireless communication, to the levitation controller.

The generated velocity profile should reflect the physical restriction because the velocity of the conveyor vehicle cannot be increased and decreased abruptly. To generate a smooth velocity profile, we adopted trapezoidal velocity profile of which acceleration is constant. In addition, it is necessary to compensate the actual position and velocity trajectories because the inverter also has a velocity control loop. For this purpose, we inserted another velocity control loop in the position control loop as shown in Figure 7.

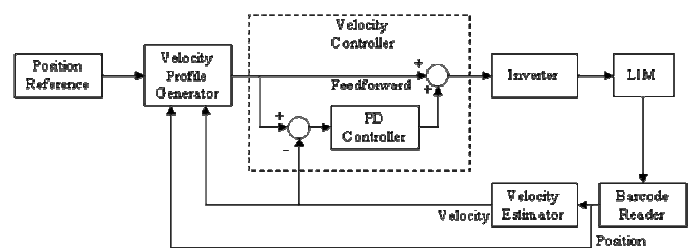


Figure 7. Block diagram of position control.

4 SIMULATIONS AND EXPERIMENTS

4.1 Results of levitation control

Some simulations and experiments were performed to verify the designed control method. In the simulation, the nonlinear force equation (4) is used. However, the parameters of the equation are estimated using FEM results rather than using their theoretical values. Equation (4) can be represented in its simplified form as

$$F(i(t), z(t)) = K \left\{ \frac{i(t) + i_{pm}}{z(t) + z_{pm}} \right\}^2 \quad (6)$$

where K , i_{pm} , and z_{pm} are appropriate constants. These parameters can be found by the least square method using FEM results. The obtained parameters are 0.0002282, 10.5502, and 0.002973, respectively.

The total weight is 792kg and the initial gap is 4.1mm, which are the measured values of the vehicle. Simulations and experiments were continued for 7 seconds: levitation starts at 1 second and stops at 5 second. In order to land off and on softly, ramp input was used as a reference trajectory. Coupling between each corner was neglected and four corners were controlled independently

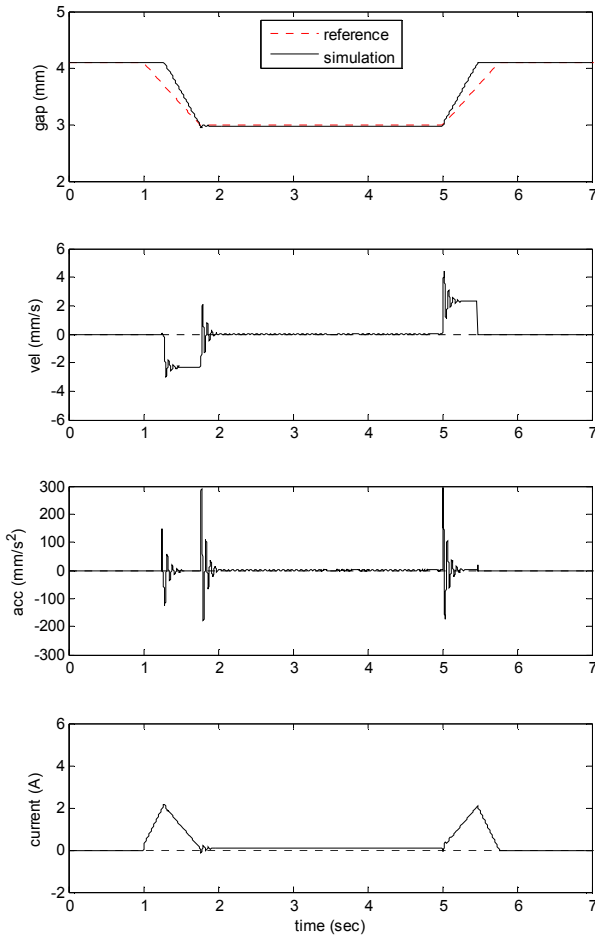


Figure 8. Simulation results (single-axis levitation).

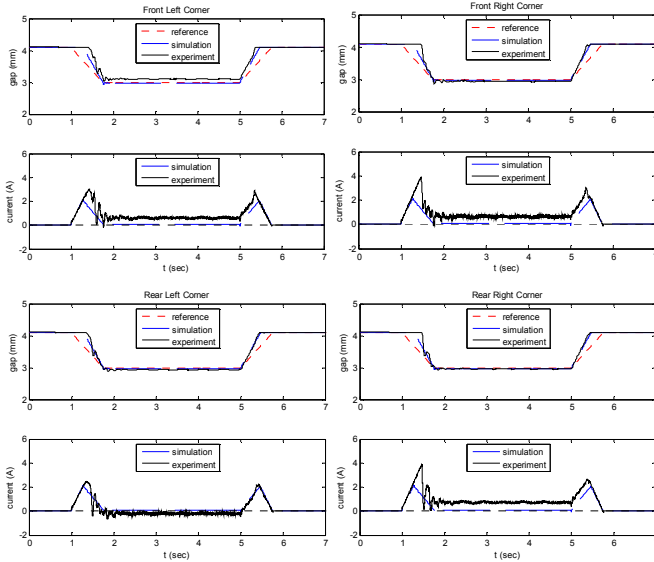


Figure 9. Experiment results (four-axis levitation).

Figure 8 shows the simulation results. Gap, its first and second derivatives (velocity and acceleration) are depicted as well as the coil current. The results of a single-axis are given, and the gap is tracking the reference gap with a quite good accuracy. The

required current for landing on and off is less than 2A, and the steady-state current has small positive value near zero.

In figure 9, experiment results are shown. Gap trajectories and coil currents of all corners are given. For the comparison, the above simulation results are also included in each figure. As a whole, the experiment results are similar to the simulation results. However, the required currents differ from each other and are increased slightly. Unbalanced weight distribution and increased weight are main causes of these observations. It is also considered that right sides are heavier than left sides because more currents are required.

4.2 Results of position control

Propulsion experiments were performed to validate the trapezoidal velocity profile and the performance of the position control. The acceleration is set to 0.5m/s^2 and the maximum velocity is set to 1m/s in the experiment. The vehicle is commanded to move from 3m to 12m.

Figure 10 shows the results of the position control. The absolute position of the vehicle and measured velocity are shown in the figure, and the zoom-in graph is also given to recognize the tracking accuracy. The measured velocity profile has a trapezoidal shape and about 26mm overshoot is observed near the final position. The final tracking error is maintained within -1mm .

It is observed that the vehicle is accelerated with the given acceleration in the acceleration period, but the vehicle is decelerated slowly in the deceleration period. It is because the control algorithm is modified to improve the tracking performance.

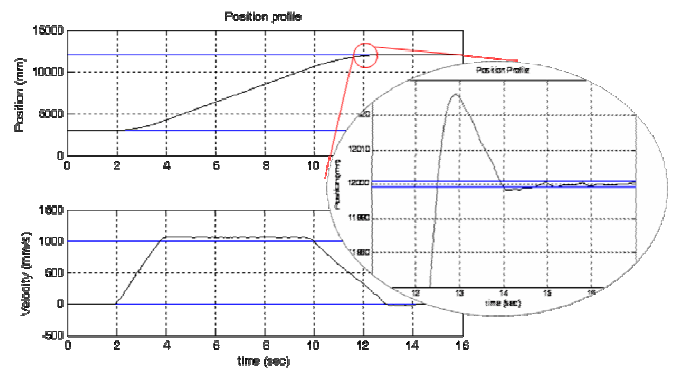


Figure 10. Experiment results (four-axis levitation).

5 CONCLUSIONS

In this paper, a magnetically levitated LCD glass conveyor system, of which payload is 350kg, is developed. The levitation and thrust systems are newly designed, and control of both systems is implemented. From the simulations and experiments, the stability of the levitation and the tracking performances of the position control are verified. Due to the use of the PM, the conveyor vehicle can be levitated with less current and the generated particles can be reduced because of the contactless operation.

Future works include the enhancement of the levitation stability and vibration characteristics. It is necessary to reduce the overshoot and improve the accuracy of the position control.

6 REFERENCES

- Kim, C.H., Lee, J.M., Han, H.S., Kim, B.S. and Kim, D.S. 2011. Development of magnetically levitated LCD glass conveyor, *8th International Symposium on Linear Drives for Industrial Applications*, Eindhoven, The Netherlands, July 3-6, 2011.
- Kim Y.H., Kim K.M. and Lee J. 2001. Zero power control with load observer in controlled-PM levitation, *IEEE Trans. On Magnetics* 37(4): 2851-2854.
- Mizuno T. and Takemori Y. 2002. A transfer-function approach to the analysis and design of zero-power controllers for magnetic suspension systems, *Electrical Engineering in Japan* 141(2): 116-132.
- Morishita M., Azukizawa T., Kanda S., Tamura N. and Yokoyama T. 1989. A new maglev system for magnetically levitated carrier system, *IEEE Trans. On Vehicular Technology* 38(4): 230-236.
- Sun F. and Oka K. 2009. Zero power non-contact suspension system with permanent magnet motion feedback, *J. System Design and Dynamics* 3(4): 627-638.
- Sung H.K., Jho J.M., Lee and Kim D.S. 2006. A study on gap treatment in EMS type maglev, *Autumn Conf. of the Korean society of railway*, Gyeongsangnam-do, Korea, November 9-10, 2006.
- Tzeng Y.K. and Wang T.C. 1995. Dynamic analysis of the maglev system using controlled-PM electromagnets and robust zero-power-control strategy, *IEEE Trans. On Magnetics* 31(6): 4211-4213.